Available online at www.sciencedirect.com
SciVerse ScienceDirect
Physics Procedia 36 (2012) 1031 – 1036
Physics Procedia

Superconductivity Centennial Conference

Design of an HTS levitated double-sided HTSLSM for maglev

Luhai Zheng[a], Jianxun Jin[a]*, Youguang Guo[b], Jianguo Zhu[b]

[a]*University of Electronic Science and Technology of China, Chengdu 611731, China*
[b]*Faculty of Engineering and Information Technology, University of Technology Sydney, Sydney, NSW 2007, Australia*

Abstract

A hybrid high temperature superconducting (HTS) linear synchronous propulsion system composed of a double-sided HTS linear synchronous motor (HTSLSM) in the middle and HTS magnetic suspension sub-systems on both sides has been proposed for a middle-low-speed maglev. Three carriages has been made up for the proposed maglev, and each carriage consists of four HTSLSM modules. The HTSLSM has been designed to reach a speed of 69 km/h and a maximum thrust of 48.9 kN for each motor. The finite element analysis has been used for the theoretical verification. The results obtained show that the HTS linear propulsion system satisfies the principal requirements for the maglev.

PACS: 85.25.Ly
Keywords: High temperature superconductors (HTS), HTS linear synchronous motor, HTS magnetic suspension, HTS bulk, maglev.

1. Introduction

There are two important applications of high temperature superconducting (HTS) bulk for linear motors, i.e. the linear synchronous driving and magnetic suspension. Recently, some HTS linear synchronous motors (HTSLSMs) with field-cooled (FC) or zero-field-cooled (ZFC) HTS bulks as the secondary have been studied and developed [1-7], and HTS magnetic suspension systems with various permanent magnet guideways (PMGs) have also been built [8-11]. Among them, hybrid HTS linear synchronous propulsion systems for the maglev using a single-sided HTSLSM for propulsion and HTS magnetic suspension sub-systems on both sides for the mover suspension [3,4], and using a double-sided

* Corresponding author. Tel./fax: +86-28 61830798
E-mail address: jxjin@uestc.edu.cn.

1875-3892 doi:10.1016/j.phpro.2012.06.101

HTSLSM for propulsion and an HTS magnetic suspension sub-system located on the bottom of the HTSLSM for the mover suspension were developed and experimentally studied [5], which present both the advantages of HTS linear driving and HTS magnetic suspension techniques. However, their thrust and suspension forces cannot satisfy the practical requirements well simultaneously for using a single-sided HTSLSM or one HTS magnetic suspension sub-system.

In this paper, a new hybrid HTS linear synchronous propulsion system for the maglev is proposed, which is propelled by double-sided HTSLSMs and suspended by HTS magnetic suspension sub-systems on both sides of the HTSLSMs. This structural arrangement makes the maglev produce stable thrust and suspension forces simultaneously with simple control system. As one demonstrator model for a middle-low-speed maglev, the HTS linear propulsion system is composed of three carriages, and each carriage consists of four HTSLSM modules. For the double-sided HTSLSM, a 2D finite element analysis (FEA) model has been built up for the dynamic simulation. As results, the starting characteristics and the thrust performance of the HTSLSM have been obtained with an optimal design on the secondary HTS bulk magnet, which have verified the theoretic analysis and the feasibility of applying the HTS linear synchronous propulsion system for the maglev.

2. HTS magnetic suspension propulsion system model

The HTS linear synchronous propulsion system with one HTSLSM module is shown in Fig. 1, where the double-sided HTSLSM is located in the middle and two HTS magnetic suspension sub-systems connected to the secondary mover are installed on both sides of the HTSLSM. The primary winding of the HTSLSM is designed modularly as illustrated in Fig. 2. As shown, each module is made up of three concentrated windings assembled on one nonmagnetic support, so that the double-sided primary stator can be installed easily. The secondary is composed of 32 pulse magnetized YBCO (Y-123) HTS bulk magnets, which form 8 alternating magnetic poles along the moving direction, and 4 poles of same polarity installed side by side along transverse direction for each magnetic pole.

In order to obtain the secondary HTS bulk magnet array with alternating magnetic poles easily, a split HTS coil pulse magnetization system is designed as shown in Fig. 3, which is assembled on both sides of the double-sided primary stator, resulting in that the HTSLSM can run readily after the secondary have been magnetized. The HTS magnetic suspension sub-system consists of FC YBCO bulks and PMG as its track as shown in Fig. 1. The main design parameters of the HTSLSM are listed in Table 1.

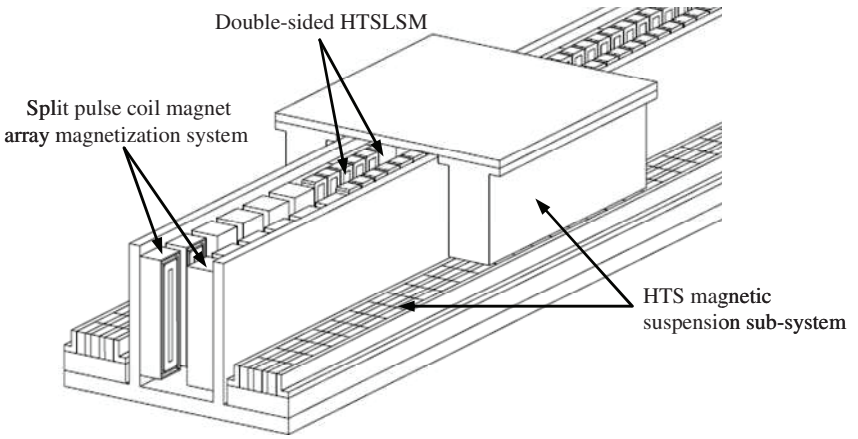

Fig. 1. Model of maglev with double-sided HTSLSM driving and HTS magnetic suspension sub-systems

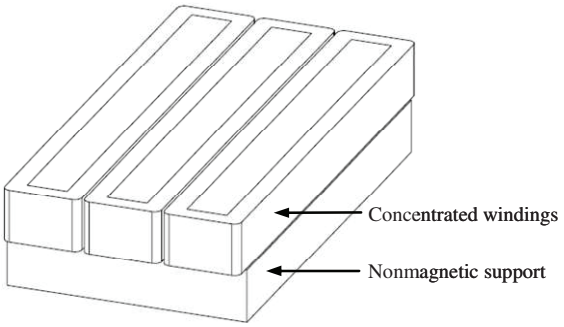

Fig. 2. Module of primary winding

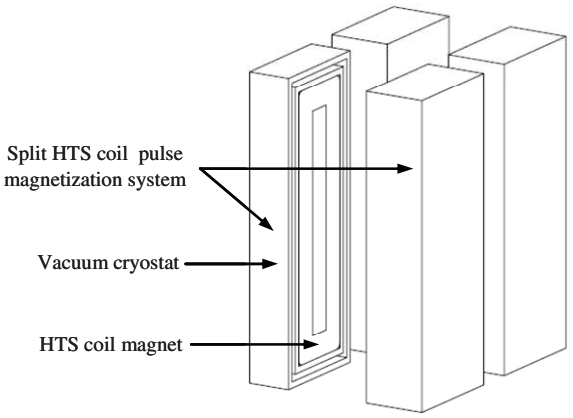

Fig. 3. Structure of the split HTS coil pulse magnetization system

Table 1. Dimensions and parameters of the HTSLSM

Primary	Slot length w_{sl} (y-direction)	32 mm
	Slot depth h_{sl}	45 mm
	Tooth length l_t (y-direction)	32 mm
	Tooth width w_t (z-direction)	320 mm
	Tooth pitch y_1	64 mm
	Pole pitch τ	96 mm
	Turns of one winding N_1	3
Secondary HTS bulk magnets	Length l_s (y-direction)	80 mm
	Width w_s (z-direction)	80 mm
	Height h_s (x-direction)	40 mm
	Trapped magnetic flux density	1 T
	Relative permeability μ_r	0.4
	Number along y-direction	8
	Number along z-direction	4
Operational parameters	Rated speed v_s	69 km/h
	Rated frequency f	100 Hz
	Maximum thrust F_{em_max} (one module)	48.9 kN
	Power factor cosφ	0.96

3. Performance analysis of HTSLSM by FEA method

3.1. FEA model and starting characteristics

According to the geometric parameters as listed in Table 1, a 2D FEA model of the HTSLSM is built up by using Ansoft Maxwell software as shown in Fig. 4. Based on this model, the running characteristics of the HTSLSM can be simulated and obtained using time-stepping transient analysis method. When the HTSLSM is set at the rated working conditions including the exciting frequency of 100 Hz, the flux

linkage distributions at different time is shown in Fig. 5, and Fig. 6 plots the starting characteristics versus time. As it can be seen from Fig. 6, the displacement of the secondary mover increases linearly with time, and its speed fluctuates around 19.2 m/s (= 69.12 km/h), and the fluctuation is caused by the starting impact currents as shown in Fig. 7(a). Fig. 7(a) depicts the phase A current at the starting stage, which shows that the maximum impact current is about 2.3 time that of the rated current, resulting in a large impact thrust as shown in Fig. 7(b). Therefore, in the practical application, an optimal control strategy is necessary to be applied to decrease the impact current to obtain a better starting performance.

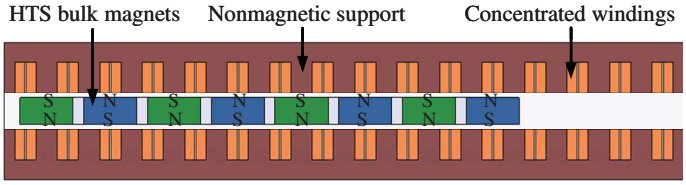

Fig. 4. FEA model of the double-sided HTSLSM

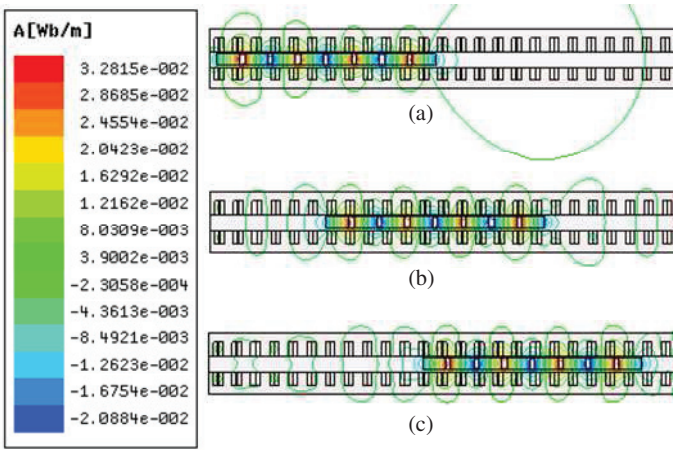

Fig. 5. Distribution of flux linkage at different time under f = 100 Hz: (a) t = 0 s; (b) t = 0.018 s; (c) t = 0.036 s

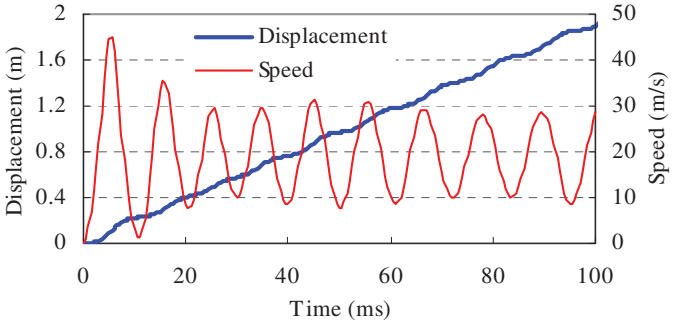

Fig. 6. Displacement versus time at rated conditions (f = 100 Hz)

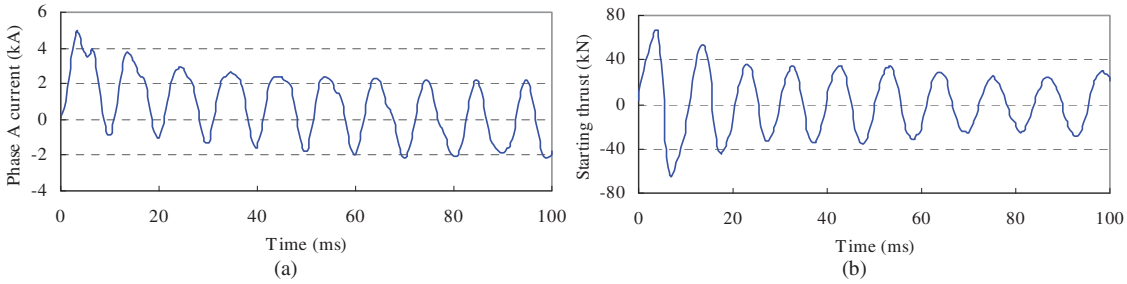

Fig. 7. Starting characteristics: (a) starting phase A winding under rated conditions; (b) starting thrust under rated conditions

3.2. Thrust performance and the size optimization of HTS bulk magnet

The electromagnetic air gap length L_{gap} has important influence on the thrust. The locked-mover thrusts of the HTSLSM are calculated for different L_{gap} as shown in Fig. 8(a), where the amplitudes of the thrust waveforms are the maximum thrust F_{em_max}. As can be seem from the figure, the F_{em_max} increases nearly linearly as L_{gap} decreases, and when the L_{gap} decreases from 20 mm to 6 mm, the F_{em_max} increases from 37.1 kN to 51.7 kN with the rated thrust equal to 48.9 kN under the L_{gap} of 8 mm.

However, when the L_{gap} is bigger than a critical value g_c, the HTSLSM can not start normally, and the pole arc coefficient a_i (the length of HTS bulk magnet L_{bulk} / pole pitch τ) has substantive influence on the value of g_c. Fig. 8(b) illustrates the allowed maximum g_c versus a_i, showing that g_c increases with a_i until it reaches its peak value of 25 mm under $a_i = 0.96$. In the calculations, the ratio of the height of HTS bulk H_{bulk} to the length of the HTS bulk L_{bulk} is kept to a constant value b (=H_{bulk} / L_{bulk}) of 0.5.

The ratio of b also has important impact on the thrust of HTSLSM. Fig. 9(a) shows the F_{em_max} versus a_i for different ratio of b. From the figure, when the a_i is smaller than a critical value a_{i_c}, the HTSLSM can not start normally as shown in Fig. 9(a) under $b = 0.5$. When the a_i is bigger than the critical value, the F_{em_max} increases linearly with a_i, and the bigger the b, the smaller the a_{i_c} can be obtained. When the $b = 1$, the a_{i_c} is about 0.56; however, when the $b = 0.3$, the a_{i_c} is limited to 0.85.

Fig. 9(b) shows the F_{em_max} versus the ratio of b under different length of HTS bulk, which shows that if the $b < 0.35$ for the HTS bulk with a length of 80 mm, the motor cannot start normally. When the $b \geq 0.35$, the motor is able to start and run well, and the F_{em_max} increases almost linearly with b. The bigger a_i results in that the smaller b can be allowed. When the $a_i = 1$, the smallest value of b is 0.3, namely the allowed minimum thickness of HTS bulk $H_{bulk\_c} = 28.8$ mm. Moreover, the smaller a_i leads to the smaller H_{bulk_c}.

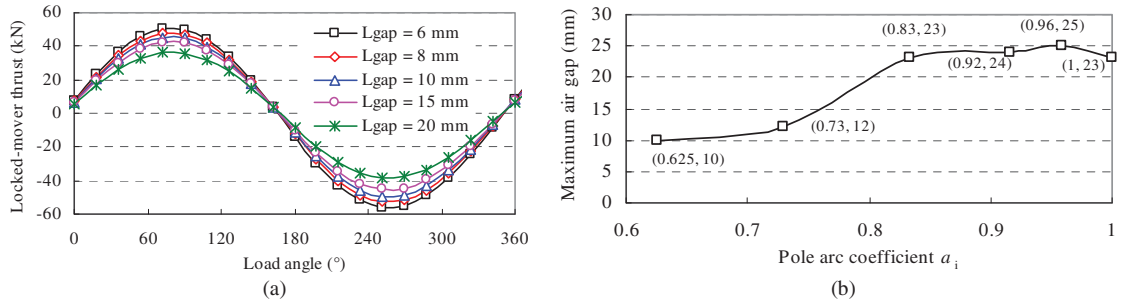

Fig. 8. (a) Locked-mover thrust characteristics under different air gap length; (b) Allowed maximum air gap under different pole arc coefficient a_i of HTS bulk magnet

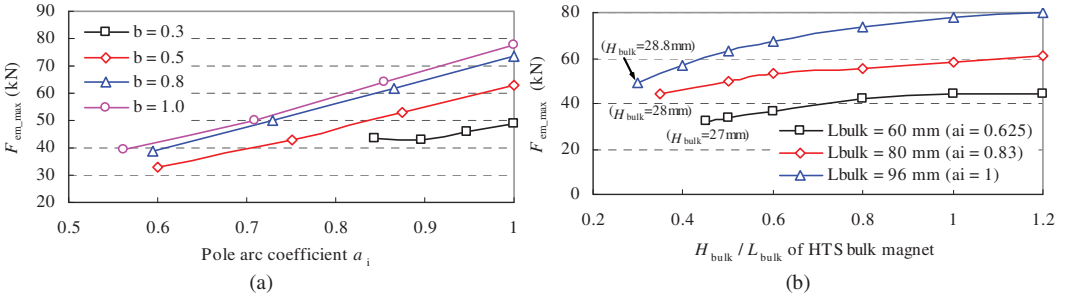

Fig. 9. The influence of size of HTS bulk magnet on thrust: (a) F_{em_max} versus pole arc coefficient α_i for different values of b (=H_{bulk} / L_{bulk}); (b) F_{em_max} versus b of HTS bulk magnet with different length L_{bulk}

4. Conclusions

An HTS linear synchronous propulsion system composed of a double-sided HTSLSM and HTS magnetic suspension sub-systems on both sides for the maglev has been designed and studied. The results obtained by the time-stepping transient analysis on a built 2D FEA model of the double-sided HTSLSM show that the propulsion system can start normally and run well at rated conditions, and a speed of 69 km/h and the maximum thrust of 48.9 kN can be obtained for each motor module. The results obtained from the optimal design on the HTS bulk magnets are essential to select an optimal HTS bulk for the practical application to have a better propulsion performance suitable for the middle-low-speed maglev.

References

[1] K. Yoshida, H. Matsumoto and M. Eguchi. Optimal design of thrust force in vertical-type HTS bulk LRM. *Physica C* 426-431(2005)839.

[2] R. Muramatsu, S. Sadakata, M. Tsuda and A. Ishiyama. Trial production and experiments of linear actuator with HTS bulk secondary. *IEEE Trans. Appl. Superconduct.* 11(2011)1976.

[3] J. X. Jin and L. H. Zheng. Driving models of high temperature superconducting linear synchronous motors and characteristic analysis. *Superconduct. Sci. Tech.* 24(2011)055011.

[4] J. X. Jin, L. H. Zheng, Y. G. Guo, W. Xu and J. G. Zhu. Analysis and experimental validation of an HTS linear synchronous propulsion prototype with HTS magnetic suspension. *Physica C* 471(2011)520.

[5] J. X. Jin, L. H. Zheng, W. Xu, Y. G. Guo and J. G. Zhu. Thrust characteristic of a double-sided HTSLSM with an HTS magnetic suspension system. *J. Appl. Phy.* 109(2011)073916.

[6] G. Stumberger, M. T. Aydemir and A. L. Thomas. Design of a linear bulk superconductor magnet synchronous motor for electromagnetic aircraft launch systems. *IEEE Trans. Appl.* Superconduct. 14(2004)54.

[7] A. Sato, H. Ueda and A. Ishiyama. Operational characteristics of linear synchronous actuator with field-cooled HTS bulk secondary. *IEEE Trans. Appl. Superconduct.* 15(2005)2234.

[8] J. S. Wang, S. Y. Wang, Y. Zeng, H. Y. Huang, F. Luo, Z. P. Xu, et al. The first man-loading high temperature superconducting maglev testvehicle in the world. *Physica C* 378–381(2002)809.

[9] J. X. Jin, Y. G. Guo and J. G. Zhu. Principle and analysis of a linear motor driving system for HTS levitation applications. *Physica C* 460-462(2007)1445.

[10] L. Schultz, O.de Haas, P. Verges, C. Beyer, S. Rohlig, H. Olsen, et al. Superconductively levitated transport system - the SupraTrans project. *IEEE Trans. Appl. Superconduct.* 15(2005)2301.

[11] K. L. Kovalev, S. M. A. Koneev, V. N. Poltavec and W. Gawalek. Magnetically levitated high-speed carriages on the basis of bulk HTS elements. Pro. 8th Intern. Symp. Magn. Susp. Technol. (ISMST'8), Dresden, Germany, p. 51, 2005.